Amphiphilic Dextran Derivatives Nanoparticles for the Delivery of Mitoxantrone

Huan Wang,[1,2] Siyuan Han,[1,2] Jihong Sun,[2] Tengfei Fan,[1] Cixia Tian,[1] Yan Wu[1]

[1]*National Center for Nanoscience and Technology, Laboratory of Nanobiomedicine and Nanosafety, Division of Nanomedicine and Nanobiology, Beijing, China, No. 11 Beiyitiao, Zhongguancun, Beijing 100190, China*
[2]*College of Environmental and Energy Engineering, Beijing University of Technology, Beijing 100124, China*

Received 14 November 2010; accepted 11 November 2011
DOI 10.1002/app.36534
Published online in Wiley Online Library (wileyonlinelibrary.com).

ABSTRACT: In this work, biodegradable amphiphilic copolymer nanoparticles based on dextran, polylactide (PLA), and 1,2-dipalmitoyl-*sn*-glycero-3-phosphoethanolamine (DPPE) were prepared. To estimate their feasibility as drug carriers, an antitumor model drug, mitoxantrone (MTO), was successfully incorporated into the polymeric nanoparticles by double-emulsion (DE) and nanoprecipitation (NP) methods. The MTO-loaded nanoparticles were confirmed by dynamic light scattering and transmission electron microscopy. The MTO-loaded nanoparticle size, size distribution, and encapsulation efficiency were influenced by the feed weight ratio of the copolymer to MTO. In addition, *in vitro* release experiments showed that the release behavior was affected by the fabrication method and the pH of the release media. The MTO-loaded nanoparticles showed faster release by the NP method and at pH 5.4 than by the DE method and in pH 7.4 buffer. The dextran–PLA–DPPE polymeric nanoparticles could be useful as drug carriers for antitumor drug delivery. © 2012 Wiley Periodicals, Inc. J Appl Polym Sci 000: 000–000, 2012

Key words: copolymers; drug delivery systems; nanoparticle

INTRODUCTION

Amphiphilic copolymers consisting of hydrophilic and hydrophobic segments can form micelle structures with a hydrophobic inner core and a hydrophilic outer shell in aqueous media.[1–4] Polymeric micelles have received special attention because of their potential applications and academic appeal in many interdisciplinary fields.[5–7] These core–shell type micelles may be used as drug-delivery vehicles for poorly water-soluble drugs, especially when the micelles are made with suitable biodegradable polymers.

Dextran is a natural polysaccharide. It has unique physicochemical properties, such as a high water solubility and a large number of hydroxyl groups, which make dextran convenient for modification.[8–11] Furthermore, its excellent biocompatibility, biodegradability, and noncytotoxicity have made dextran widely used in biological medicine as a biomaterial. Amphiphilic copolymers based on dextran-modified hydrophobic molecules tend to form nanosized micelles in water by self-assembly.

Polylactide (PLA) is a kind of biodegradable materials with a low toxicity, excellent biocompatibility, and bioabsorbability *in vivo*. It has been widely used in biomedical applications, such as sustained drug-delivery systems, implants for orthopedic devices, and absorbable fibers.[12,13] However, the low hydrophilicity and high crystallinity of PLA result in poor soft-tissue compatibility.[14] Recently, many researchers have reported the synthesis of PLA-grafted dextran by a three-step method.[15,16]

Dipalmytoylphosphatidylethanolamine (DPPE) is the main constituent of the inner membrane. Some articles have reported that poly(ethylene glycol)/phosphatidylethanolamine polymers could form stable micelles in aqueous media. The characteristic size, stability, and longevity in systemic circulation make micelles containing phosphatidylethanolamine segments promising carriers for the delivery of drugs to ill sites via the enhanced permeability and retention effect.[17–20]

The aim of this work was to assess the merits of dextran–PLA–DPPE polymeric nanoparticles as drug carriers. For this purpose, the copolymer dextran–PLA–DPPE was synthesized with dextran, D,L-lactide (DLLA), and DPPE. The chemical structure and physical properties of the copolymer were characterized. Finally, mitoxantrone (MTO), an anticancer drug,[21–23] was chosen as a model drug to incorporate into the

Correspondence to: Y. Wu (wuyan66@eyou.com) or J. Sun (jhsun@bjut.edu.cn).

Contract grant sponsor: State Key Development Program for Basic Research of China (973); contract grant numbers: 2009CB930200, 2010CB934004, (863) 2007AA02Z150.

polymeric nanoparticles by the double-emulsion (DE) and nanoprecipitation (NP) methods. The drug-release behavior of the MTO-loaded polymeric nanoparticles at different pHs and fabricated by different methods was also investigated.

EXPERIMENTAL

Materials

Dextran (1500 Da), 1,2-dipalmitoyl-*sn*-glycero-3-phosphoethanolamine (DPPE), and triethylamine were purchased from Sigma Chemical Co. (St. Louis, MO, USA). DLLA, 4-nitrophenyl chloroformate (pNP), and 4-dimethylaminopyridine (DMAP) were purchased from Alfa Aesar (Ward Hill, MA, USA). MTO was purchased from Beijing HuaFeng Unite Co., Ltd. (Beijing, China). *N*-2-Hydroxyethylpiperazine-*N*′-2-ethanesulfonic acid was purchased from Beijing Bo Run Lai Te Unite Co., Ltd. (Beijing, China). All other reagents were analytical grade and were used as received.

Synthesis and characterization of the dextran–PLA–DPPE copolymer

The dextran–PLA–DPPE copolymer was synthesized by a three-step process according to our previously reported method.[24] Dextran–PLA was synthesized as follows: 10 g of DLLA was added to 500 mg of a dextran/dimethyl sulfoxide (DMSO) solution with stirring, and then, 0.5 mol of triethylamine was added dropwise. The solution was reacted at 86°C with magnetic stirring in an N_2 atmosphere. After 12 h, the reacted solution was added to ice–water, and the precipitate was collected and thoroughly washed with distilled water. Finally, the obtained crude product was extracted with toluene. The pure dextran–PLA copolymer was dried at 40°C for 48 h *in vacuo*.

The activation of dextran–PLA was performed as follows: 1.1 g of dextran–PLA was dissolved in 6 mL of chloroform with stirring, and then, 0.5 g of pNP, 40 mg of DMAP (dissolved in 6 mL of chloroform), and 1 mL of pyridine was added to the solution, and the reaction was allowed to run 0°C for 6 h and at room temperature for 12 h with magnetic stirring. The resulting product was added to ethyl ether/petroleum ether (2 : 1 v/v), and the precipitate was collected and washed with mixed ether three times. The pure product was dried *in vacuo* for 48 h.

Dextran–PLA–DPPE copolymers were synthesized as follows. A mixture of activated dextran–PLA (dextran–PLA–pNP) and DPPE [containing 0.1 mol of triethylamine, with a feed weight ratio of 20 : 1–50 : 1 (DPPE/dextran–PLA–pNP)] was suspended in 20 mL of chloroform with a magnetic stirrer at room temperature in the absence of light. After being stirred continuously for 12 h, the resulting product was added to ethyl ether/petroleum ether (2 : 1, v/v), and the precipitate was collected and washed with mixed ether three times. The dextran–PLA–DPPE copolymers were dried *in vacuo* for 48 h.

^{1}H-NMR and ^{31}P-NMR spectra were recorded on a Bruker AVANCE 400 NMR spectrometer (Billerica, MA, USA) with $CDCl_3$ or hexadeuterated DMSO as the solvent.

Thermogravimetric analysis TGA (Perkine-Elmer, Fremont, CA, USA) of the samples was conducted by TGA (PerkinElmer Instruments) at a heating rate of 20°C/min under a nitrogen atmosphere from room temperature to 900°C.

The molecular weight and molecular weight distribution were obtained by gel permeation chromatography (GPC; Waters 515-410, Milford, MA, USA; tetrahydrofuran was used as the eluent).

Preparation and characterization of the MTO-loaded dextran–PLA–DPPE copolymer nanoparticles

The MTO-loaded copolymer nanoparticles were fabricated by the DE and NP methods. The DE method was used to fabricate the nanoparticles as previously described[25] with a few changes. Briefly, 250 μL of an MTO (5 mg/mL) aqueous solution was emulsified with 1 mL of a dichloromethane (O)-containing copolymer (10 mg) by sonication (70 w) for 3 min in an ice bath. Thereafter, this first emulsion (W1) was poured into 2 mL of the PVA aqueous solution (2% w/v; W2) and sonicated (100 w) for 3 min to make W1/O/W2 DE. The DE was diluted in 10 mL of PVA solution (0.6% w/v), and the dichloromethane was rapidly eliminated by a rotary evaporator under reduced pressure. Finally, the nanoparticles were collected by centrifugation at 13,000 rpm for 10 min and washed twice with deionized water before lyophilization.

The NP technique[26] was developed for comparison with the DE method. Briefly, 1.5 mL of the copolymer solution in acetone (10 mg/mL) was added dropwise to 10 mL of water with 100 μL of MTO (5 mg/mL) under magnetic stirring for 30 min. Acetone was eliminated by evaporation under reduced pressure. The MTO-loaded nanoparticles were collected by centrifugation at 13,000 rpm for 10 min and then washed with deionized water three times.

The morphology of the nanoparticles was observed with transmission electron microscopy (TEM; FEI, Tecnai G^{2}20, Hillsboro, Oregon, USA). A drop of the suspension of the nanoparticles was placed onto a copper grid with carbon film. After deposition for about 2 min, the grid was tapped with filter paper to remove surface water and then air-dried. The samples on the grid were stained with uranyl acetate and air-dried before the measurement.

The particle size and size distribution were measured by a Zetasizer NanoZS analyzer (Malvern Instruments Ltd., Malvern, UK) with the dynamic light scattering (DLS) technique. Before measurement, the nanoparticles were appropriately diluted with distilled water.

The encapsulation efficiency (EE) was determined by measurement of the MTO concentration in the supernatant with a UV spectrophotometer (PerkinElmer Lambda 850) at 660 nm. EE was calculated from the following equation:

$$\text{EE } (\%) = W_0 - W_t/W_0 \times 100\%$$

where W_0 is the weight of initial MTO and W_t is the MTO concentration in the supernatant. Each sample was assayed in triplicate.

Physical stability of the MTO-loaded dextran–PLA–DPPE nanoparticles

The MTO-loaded dextran–PLA–DPPE nanoparticles (DE and NP methods; 2 mg/mL) were determined for physical stability in phosphate buffered saline (PBS) at 25°C. Nanoparticle diameter changes as a function of time and the scattering intensities were evaluated by the DLS technique, as mentioned previously.

Dilution experiment with the MTO-loaded dextran–PLA–DPPE nanoparticles

The dilution experiment was carried out as follows: 1 mL of MTO-loaded dextran–PLA–DPPE nanoparticles were withdrawn, and then, we added HEPES buffer solution (5 mmol/L N-2-hydroxyethylpiperazine-N-2-ethanesulfonic acid, 0.9% NaCl, pH 7.0) to dilute the MTO-loaded dextran–PLA–DPPE nanoparticles. The concentration of the MTO-loaded dextran–PLA–DPPE nanoparticles was diluted to 1 g/L. Then, 50 μL of the MTO-loaded dextran–PLA–DPPE nanoparticles were taken out and diluted with the HBS buffer solution by 10, 100, and 1000 times, respectively. At selected time intervals (2, 6, and 12 h), the previously diluted solution (100 μL) was extracted and centrifuged at 13,000 rpm for 10 min. The MTO concentration in the supernatant was calculated on the basis of the absorbance intensity at 660 nm, and the drug EE was determined as mentioned previously.

In vitro drug-release profiles

In vitro drug-release from the nanoparticles was carried by a dialysis method. The MTO-loaded nanoparticles (DE and NP methods) were dispersed in 5 mL of deionized water and then transferred into the dialysis bag (molecular weight cutoff = 12,000 Da). The dialysis bags were incubated in 35 mL of incubation media (PBS, pH 7.4) at 37°C and shaken at 105 rpm in a water bath. At the predetermined time intervals, 3-mL samples were withdrawn for analysis by a UV/visible spectrophotometer (660 nm), and 3 mL of fresh PBS was added to replace the withdrawn amount. Particularly for the effect of pH on the release rate of MTO, the MTO-loaded nanoparticles were dispersed in 5 mL of deionized water and then transferred into dialysis bags (12,000 Da). The dialysis bags were incubated in 35 mL of different incubation media (PBS, pH 7.4 or 5.4) at 37°C and shaken at 105 rpm in a water bath. At the predetermined time intervals, 3-mL samples were withdrawn for analysis by spectrophotometry, and 3 mL of fresh PBS was added to replace the withdrawn amount. For comparison, the release of free MTO was also performed in different PBSs (pH 7.4 or 5.4) at 37°C. The released MTO was analyzed by UV/visible spectrophotometry at 660 nm.

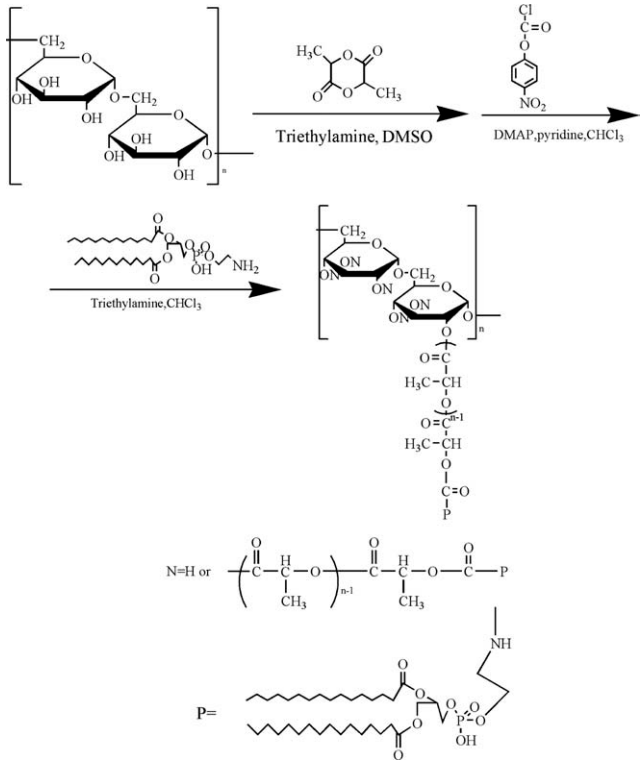

Scheme 1 Synthetic route of the dextran–PLA–DPPE copolymer.

RESULTS AND DISCUSSION

Synthesis and characterization of the dextran–PLA–DPPE copolymer

The dextran–PLA–DPPE copolymer was synthesized by a three-step processes. The polymerization route of the dextran–PLA–DPPE copolymer is shown in Scheme 1. Fist, the dextran–PLA copolymer was synthesized by the one-step ring-opening polymerization

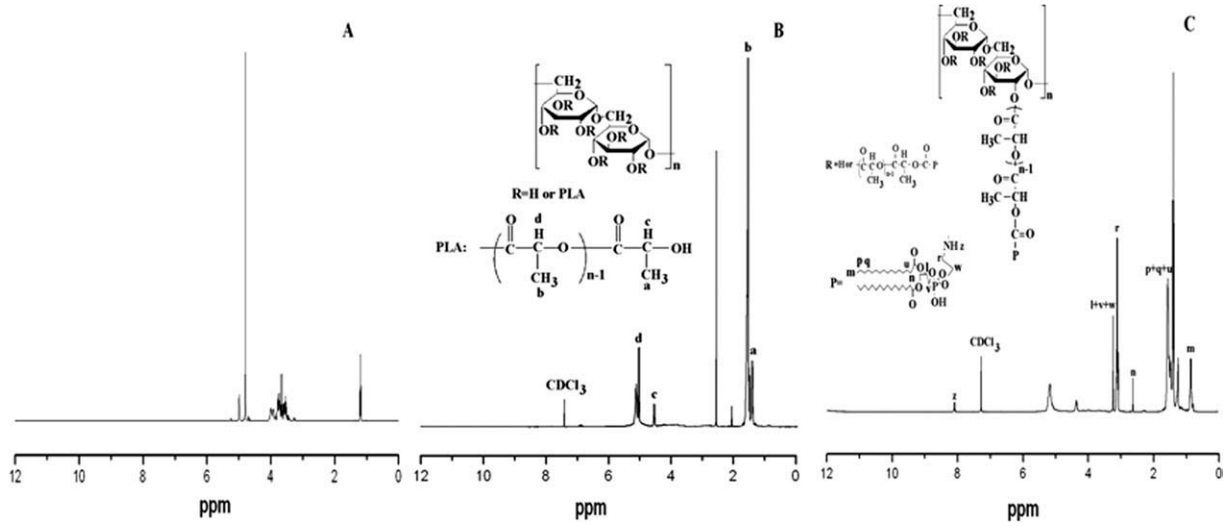

Figure 1 ^{1}H-NMR spectra of (A) dextran, (B) dextran–PLA, and (C) dextran–PLA–DPPE (20 : 1).

of DLLA and dextran in the presence of triethylamine. Then, the dextran–PLA was activated by pNP. Finally, the dextran–PLA–DPPE copolymers were synthesized by adjustment of the ratio of DPPE to dextran–PLA–pNP. The weight-average molecular weight of dextran–PLA was 1.44×10^4 Da, and the polydispersity was 1.25 (determined by GPC). The different samples, named dextran–PLA–DPPE 20 : 1 (where the numbers indicate the feed weight ratio of DPPE to dextran–PLA–pNP) and dextran–PLA–DPPE 50 : 1 were synthesized, respectively. The weight-average molecular weights of the dextran–PLA–DPPE copolymers were 2.87×10^4 and 3.83×10^4 Da, and the polydispersities were 1.40 and 1.53 (determined by GPC), respectively. The copolymers of dextran–PLA and dextran–PLA–DPPE had relatively narrow molecular weight distributions. With the increase of DPPE content, the dextran–PLA–DPPE copolymer molecular weight increased. The introduction of the DPPE segment led to an increase in the molecular weight of the dextran derivative. This indicated that higher the content of DPPE was, the greater the opportunity was for DPPE to react with the dextran–PLA–pNP reactive center. The final products of dextran–PLA–DPPE had good solubility in $CHCl_3$, DMSO, and tetrahydrofuran.

The basic chemical structure of dextran and its copolymer was studied by ^{1}H-NMR and ^{31}P-NMR.

Figure 1(A–C) shows the ^{1}H-NMR spectra of dextran and the dextran–PLA and dextran–PLA–DPPE copolymers, respectively. Compared with that of dextran [Fig. 1(A)], the ^{1}H-NMR spectrum of the dextran–PLA copolymer [Fig. 1(B)] showed signals at 4.2 and 5.1 ppm, which were assigned to the methine (CH) protons of the PLA moiety located in the terminal groups and the repeat units. The signals at 1.3 and 1.6 ppm were attributed to the methyl protons of the PLA moiety located at the terminal groups and the backbones. All of these results provided evidence that the dextran derivatives contained PLA side chains. In the ^{1}H-NMR spectra of the dextran–PLA–DPPE copolymer [Fig. 1(C)], the signal at about 0.9 ppm was attributed to the terminal methyl proton of the DPPE moiety. The signal at about 8.1 ppm was assigned to the proton of —NH in the DPPE moiety. All of other absorption peaks were attributed to the protons of the DPPE moiety.[24]

Furthermore, the typical ^{31}P-NMR spectra of the DPPE and dextran–PLA–DPPE copolymer were recorded and are shown in Figure 2. Compared with that of DPPE [Fig. 2(A)], the ^{31}P-NMR spectra of the dextran–PLA–DPPE copolymer [Fig. 2(B)] showed that the peak at −0.96 ppm was generally expected for ^{31}P functionalities.[27,28] The ^{31}P-NMR spectra confirmed that the phosphate groups were chemically bonded to the material.

The thermal properties of the polymers were examined by TGA measurement. Figure 3 shows the TGA thermograms of dextran and the dextran–PLA and dextran–PLA–DPPE copolymers, respectively. Compared with dextran, the dextran–PLA and dextran–PLA–DPPE copolymers had lower thermal degradation temperatures. A fast process of weight loss appeared in the TGA curve response for the dextran–PLA and dextran–PLA–DPPE copolymers in the thermal degradation ranges. These results show that the thermal stability of the dextran–PLA and dextran–PLA–DPPE copolymers decreased relative to that of the original dextran.

Characterization of the MTO-loaded dextran–PLA–DPPE nanoparticles

The MTO-loaded copolymer nanoparticles were fabricated by the DE and NP methods. For the DE

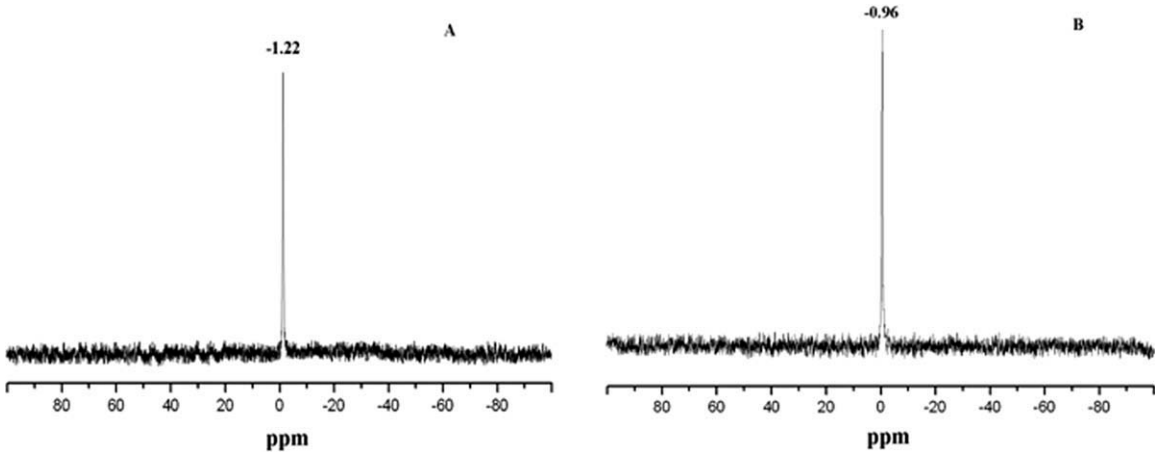

Figure 2 ^{31}P-NMR spectrum of the (A) DPPE and (B) dextran–PLA–DPPE (50 : 1) copolymer.

method, an increase in the MTO feed amount led to a decrease in EE (Table I). The difference in the osmotic pressure between the internal and external aqueous phases could have been responsible for the decrease in EE. The osmotic pressure difference did, in fact, rise with increased MTO loading and promoted an exchange between the internal and external aqueous phases, with a consequent loss of MTO. In addition, as shown in Table I, with the increase in the copolymer/MTO ratio, EE increased. This may have been because the higher the copolymer/MTO ratio was, the stronger the interaction was between the copolymer and MTO, and this may have led to more MTO being incorporated into the nanoparticles and the enhanced EE. Other experimental techniques should be paid attention during encapsulation. A rotation evaporator (RE-5203, Hangzhou Huier Instruments Ltd., Hangzhou, China) was used to reduce the evaporation time to avoid the MTO release during stirring at room temperature. Moreover, the organic solvent had to be evaporated completely because remaining organic solvent caused caking during centrifugation. The influence of drug solubility should also be considered. In this study, water-soluble MTO was chose as a model drug, and then, it was encapsulated according to the hydrophilic drug by the DE and NP methods. Its supposed mechanisms are shown in Figure 4. The good solubility of the drug facilitated more drug incorporation in the nanoparticles.

For the NP method, EE increased with increasing mass ratio of the copolymer to drug. The could be explained as was done for the DE method.

The size and size distribution of the nanoparticles prepared with various mass ratios of copolymer to MTO were examined by the DLS technique. As illustrated in Table I, for the DE and NP methods, the higher the mass ratio of copolymer to MTO was, the smaller was the mean diameter of MTO-loaded nanoparticles. The was attributed to the increase in the interaction between the copolymer and MTO with increased mass ratio of copolymer to MTO; it could form a more compact structure, so the size of

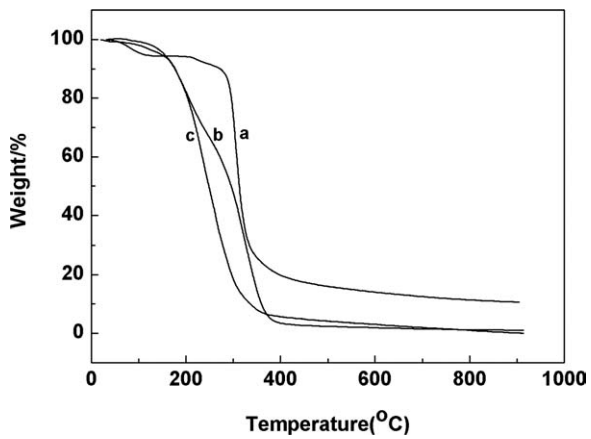

Figure 3 TGA thermograms of (a) dextran, (b) dextran–PLA, and (c) dextran–PLA–DPPE (20 : 1) copolymer.

TABLE I
Influence of the Ratio of the Copolymer to Drug on the Size, Size Distribution, and EE Values of the MTO-Loaded Dextran–PLA–DPPE Copolymer Nanoparticles[a]

Method	Copolymer/MTO mass ratio	Mean diameter (nm)	PDI	EE (%)
NP	300 : 1	160.7	0.264	87.0
	200 : 1	176.6	0.132	55.6
	100 : 1	184.7	0.072	31.5
DE	250 : 1	240.0	0.158	97.0
	200 : 1	245.1	0.129	87.8
	150 : 1	266.0	0.106	76.0
	100 : 1	290.9	0.008	67.6

[a] Dextran–PLA–DPPE (50 : 1). PDI, polydispersity. Plain NP mean diameter (nm) = 136.1, PDI = 0.088; plain DE mean diameter (nm) = 207.9, PDI = 0.024.

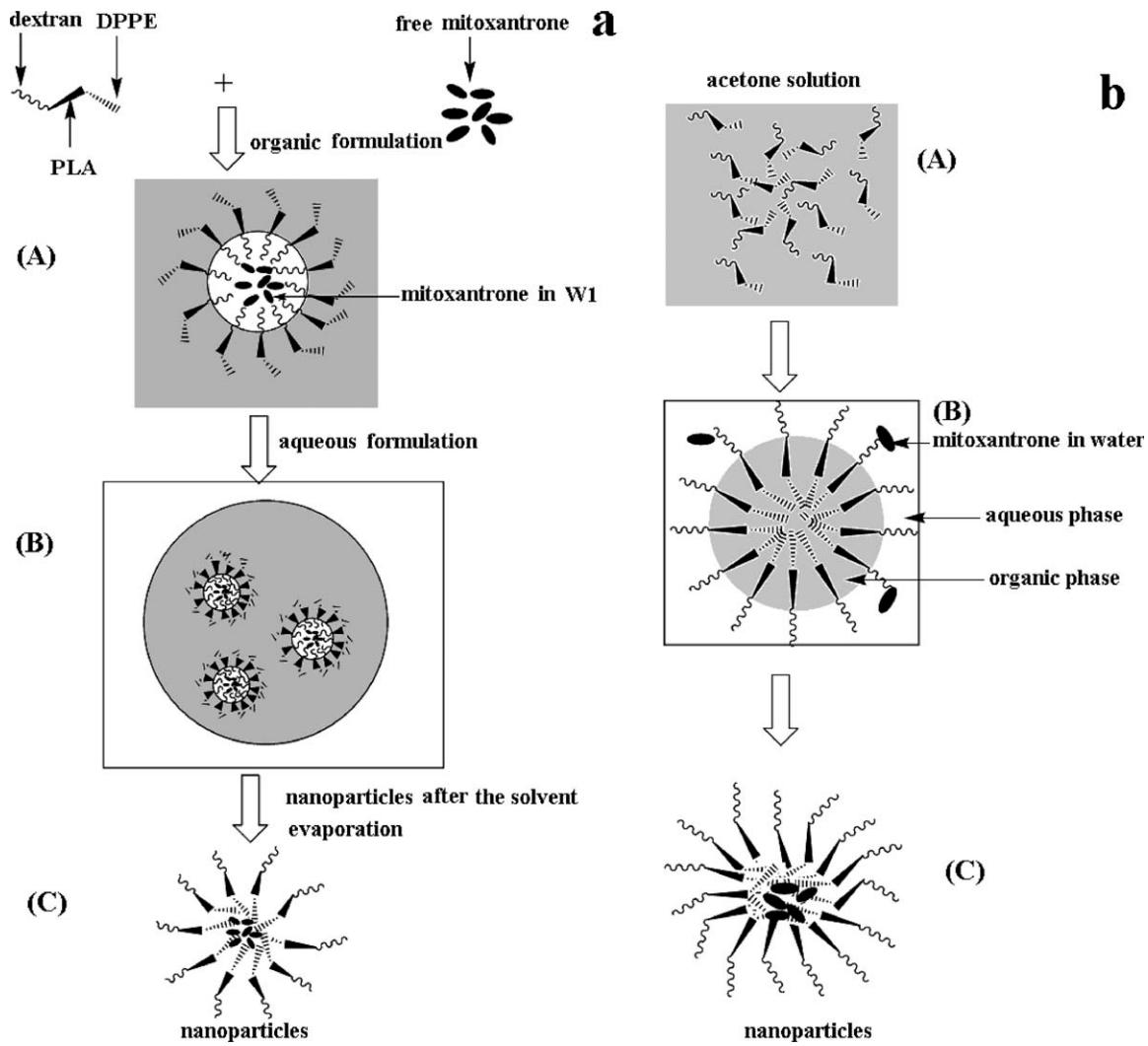

Figure 4 Supposed mechanisms of MTO encapsulation into the nanoparticles from the dextran–PLA–DPPE copolymer by both the (a) DE and (b) NP methods. DE method: (A) sonication of the dextran–PLA–DPPE copolymer dissolved in dichloromethane in the presence of an aqueous MTO solution led to the formation of a W1/O emulsion, (B) sonication of the W1/O emulsion in the presence of an outer aqueous phase gave a W1/O/W2 emulsion, and (C) nanoparticles were formed after the solvent evaporation. NP method: (A) when the solution of a dextran–PLA–DPPE copolymer in acetone was injected into an aqueous solution of MTO, the NP took place after the solvent evaporation (B).

the MTO-loaded nanoparticles decreased. The nanoparticle diameter was also influenced by the fabrication method. For the DE method, the diameters were in the range 240–291 nm. For the NP technique, the diameters were in the range 161–185 nm (Table I). Obviously, much smaller nanoparticles were formed by the NP method. This result could be interpreted in the sketch of the proposed mechanisms for the nanoparticle formations by two methods. A multinanoreservoir system was formed in the DE method, whereas a single-layer nanosphere was fabricated in the NP method (Fig. 4). Because no additives were employed in the NP method, the polydispersity range of the prepared nanoparticles was broader than that in the DE method.

The morphology and size distribution of the MTO-loaded nanoparticles formed by the NP and DE methods were determined by TEM and DLS. As shown in Figure 5(a,c), the MTO-loaded nanoparticles (copolymer/MTO = 100 : 1) were well dispersed as individual nanoparticles with a typical spherical shape. The average hydrodynamic diameters of the MTO-loaded nanoparticles prepared with a copolymer/MTO mass ratio of 100 : 1, as determined by DLS, were approximately 185 nm [Fig. 5(b)] and 291 nm [Fig. 5(d)] for the NP and DE methods, respectively, in water. The diameter observed in TEM was smaller than that detected on the Zetasizer NanoZS analyzer by the DLS technique. There was a reason that the diameter of the nanoparticles obtained by DLS reflected the hydrodynamic diameter of the nanoparticle swelling in aqueous solution, whereas that observed by TEM was the diameter of the dried nanoparticles.

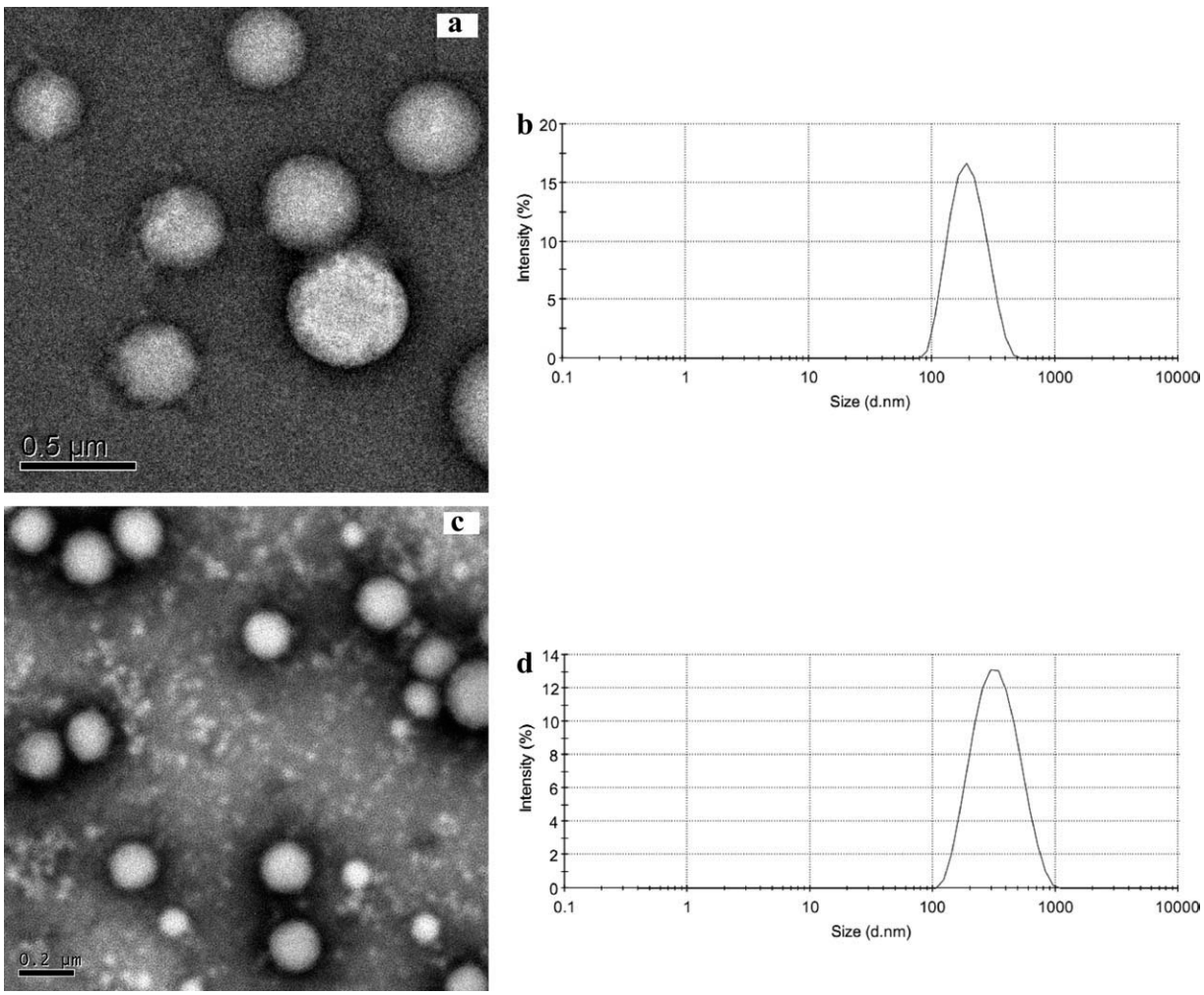

Figure 5 TEM micrograph and DLS characterization of the MTO-loaded dextran–PLA–DPPE (50 : 1) nanoparticles (copolymer/MTO 100 : 1): (a) TEM image and (b) DLS by the NP method and (c) TEM image and (d) DLS by the DE method.

Physical stability of the MTO-loaded nanoparticles

In the clinical administration of nanoparticle suspensions, vessel occlusion due to particle aggregation may occur. The steric stability of nanoparticles in the biological milieu is an important aspect to be considered. An improved steric stability of amphiphilic copolymer nanoparticles was observed in comparison with the hydrophobic PLA nanoparticles; this was attributed to the presence of hydrophilic segments on the particle surfaces to prevent a coagulation cascade. The dextran–PLA–DPPE nanoparticles had an amphiphilic structure, and the structure may have possessed a self-stabilization function. In this study, the nanoparticles were suspended in PBS, and the size changes are shown in Figure 6. Only small size variations, from 290.9 to 308.1 nm for the DE method and from 184.7 to 204.3 nm for the NP method, were observed in 16 days. The results

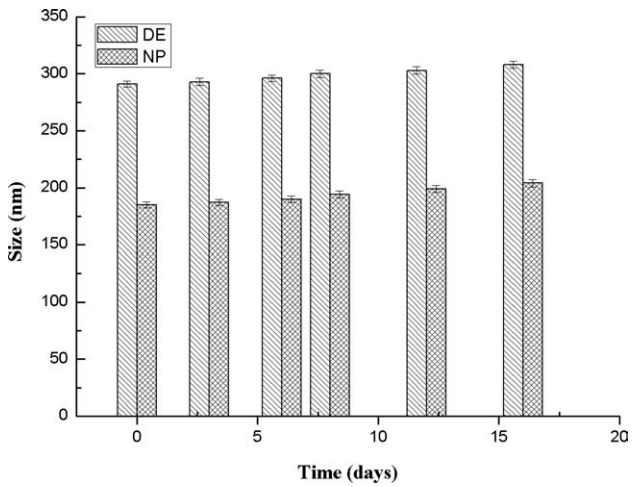

Figure 6 Steric stability of the MTO-loaded dextran–PLA–DPPE nanoparticles in PBS (DE and NP methods, copolymer/drug = 100 : 1).

TABLE II
MTO-Loaded Dextran–PLA–DPPE Copolymer Nanoparticle Resistance Dilution with HBS Solution

	EE (%) with the dilution of indicative volumes		
Time (h)	10	100	1000
2	82.7 ± 4.31	79.0 ± 3.22	78.1.± 1.29
6	81.9 ± 2.15	77.3 ± 2.69	74.8 ± 1.27
12	71.8 ± 3.04	59.6 ± 3.46	57.1 ± 2.81

DE method and copolymer/drug ratio of 100 : 1.

demonstrate that the dextran–PLA–DPPE nanoparticles possessed good steric stability *in vitro*.

Dilution experiment of the MTO-loaded dextran–PLA–DPPE nanoparticles

On intravenous administration of the drug-loaded nanoparticle solution to the body, there would be a significant dilution. This dilution would lead to the rupture of some or potentially all of the nanoparticles and the release of the encapsulated MTO. Therefore, the resistance dilution properties of the nanoparticles has important clinical value. The results of the dilution experiment are shown in Table II. In the dilution studies, the MTO-loaded dextran–PLA–DPPE nanoparticles were stable in HBS buffer solution. The MTO-loaded nanoparticles had significant resistance dilution properties. When the MTO-loaded nanoparticles were diluted with HBS solution by 1000 times and incubated for 6 h at 37°C, almost 75% of the MTO in the form of nanoparticles.

In vitro MTO release study

The appropriate release rate of MTO from the MTO-loaded nanoparticles is important for the prolonged and sustained use of the nanoparticles as drug carriers. The release profiles of MTO from the dextran–PLA–DPPE nanoparticles (by the DE and NP methods) are shown in Figure 7(A). As shown in Figure 7(A), after the initial burst, the MTO release profiles displayed a sustained fashion. The initial release burst corresponded to the diffusion of MTO located near the nanoparticle surface. This sustained release might have resulted from the diffusion of MTO into the copolymer wall and that of the MTO through the copolymer wall as well as the erosion of the copolymer.

We also observed that different fabrication methods led to different release behaviors. When we compared two fabrication methods of the polymeric nanoparticles, we found that the MTO released faster from the nanoparticles in the NP method than in the DE method. The same result previously described[29] was also observed. The copolymers were not soluble in water, and the MTO molecules dissolved in water may have been very close to the outer nanoparticle surface, forming a layer of molecules susceptible to easy and rapid release. In addition, more burst release was observed in the nanoparticles fabricated with the NP technique than in those fabricated with the DE method. This was because the different methods may have led to different distributions of MTO molecules in the nanoparticles. The fabrication method determined the amount of MTO existing near the surface of the nanoparticles. With the DE method, most of the MTO molecules were encapsulated within the nanoparticles as multinanoreservoir systems (Fig. 4). With the NP method, nanoparticles were formed as multimolecular polymeric micelles trapping MTO molecules near their outer layers (Fig. 4). Solid tumors have a weakly acidic extracellular pH (pH < 7), and cancer cells have an even more acidic pH in endosomes and lysosomes (pH 4–6).[30] Figure 7(B)

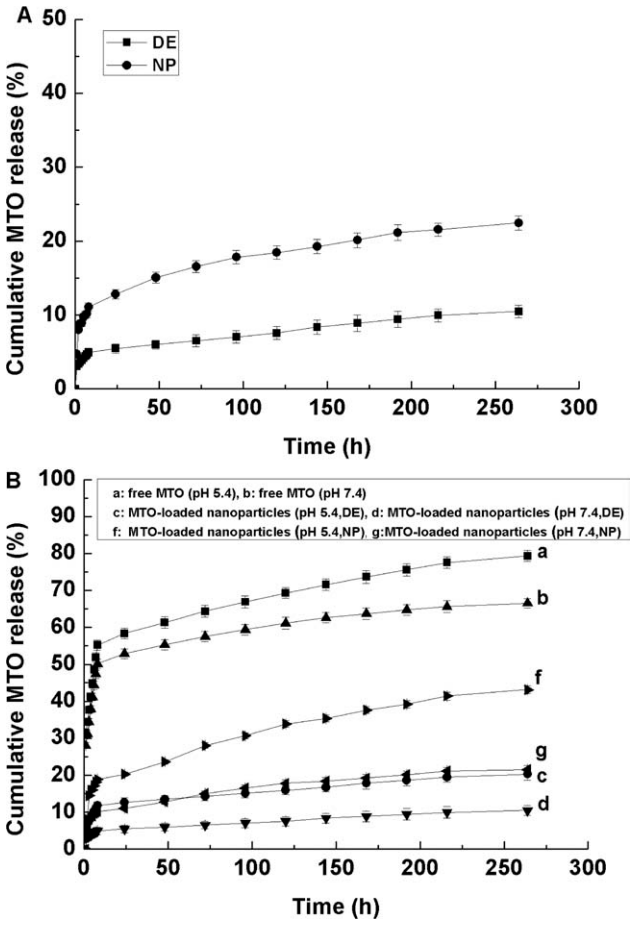

Figure 7 (A) Accumulative release of MTO from the MTO-loaded nanoparticles in pH 7.4 (DE and NP methods) and (B) accumulative release of MTO from the MTO-loaded nanoparticles (DE and NP methods, copolymer/drug = 100 : 1) in 0.1 mol/L pH 5.4 and 7.4 PBS buffer. The free MTO was used as a control.

shows the release of MTO from the nanoparticles (fabricated by the DE and NP methods) in pH 7.4 and pH 5.4 buffers. Free MTO solution was used as a control. The MTO-loaded nanoparticles exhibited slower release in both pH 7.4 and 5.4 buffers compared with the diffusion of free MTO. The much slower phase may have corresponded to the drug release due to MTO diffusion from the inner polymer matrix. Both the free MTO and MTO-loaded nanoparticles exhibited faster release in pH 5.4 buffer than in pH 7.4 buffer. This phenomenon could be explained by the fact that the protonated MTO had a higher solubility. Also, the hydrophobic interactions decreased, and electrostatic repulsion existed between the nanoparticles and MTO at pH 5.4, as discussed previously. With the NP method, the influence of different pHs (pH 5.4 and 7.4) on the *in vitro* release was more significant than with the DE method. The reason may have been the proposed mechanisms for the nanoparticle formation by two methods, as discussed earlier. The pH-sensitive properties of the nanoparticles may benefit the MTO release in tumor cells, whose pH is lower than that of normal cells.[31]

CONCLUSIONS

MTO-loaded dextran–PLA–DPPE copolymer nanoparticles were fabricated successfully by the DE and NP methods. The mass ratio of the copolymer to MTO and the fabrication method of the nanoparticles had obvious effects on the particle size and EE. The control of the nanoparticle size and EE could be achieved by optimization of the ratio of the copolymer to MTO and adjustment with different fabrication methods of the nanoparticles. The release of MTO-loaded polymeric nanoparticles exhibited pH-sensitive properties *in vitro*. This work should help in the recognition and design of new routes to antitumor drug-delivery systems.

References

1. Pan, J.; Venkatraman, S. S.; Feng, M.; Huat, L. J Controlled Release 2005, 110, 20.
2. Kato, M.; Toyoda, H.; Namikawa, T.; Hoshino, M.; Terai, H.; Miyamoto, S.; Ka, T. K. Biomaterials 2006, 27, 2035.
3. Lee, E. S.; Kim, D.; Youn, Y. S.; Bae, Y. H. J Controlled Release 2007, 123, 19.
4. Kaminski, M. D.; Xie, Y. M.; Mertz, C. J.; Finck, M. R.; Chen, H.; Rosengart, A. J. Eur J Pharm Sci 2008, 35, 96.
5. Kwon, G. S.; Kataoka, K. Adv Drug Delivery Rev 1995, 16, 295.
6. Xu, R.; Winnik, M. A.; Hallet, F. R.; Riess, G.; Croucher, M. D. Macromolecules 1991, 24, 87.
7. Forrest, M. L.; Won, C. Y.; Malick, A. W.; Kwon, G. S. J Controlled Release 2006, 110, 370.
8. Cai, Q.; Yang, J.; Bei, J. Z.; Wang, S. G. Biomaterials 2002, 23, 4483.
9. Ouchi, T.; Saito, T.; Kontani, T.; Ohya, Y. Macromol Biosci 2004, 4, 458.
10. Ouchi, T.; Kontani, T.; Ohya, Y. J Polym Sci Part A: Polym Chem 2003, 41, 2462.
11. Ouchi, T.; Kontani, T.; Ohya, Y. Polymer 2003, 44, 3927.
12. Perez, C.; Sanchez, A.; Putnam, D.; Ting, D.; Langer, R.; Alonso, M. J Controlled Release 2001, 75, 211.
13. Baras, B.; Benoit, M. A.; Gillard, J. Int J Pharm 2000, 200, 133.
14. Suh, H.; Hwang, Y. S.; Lee, J. E.; Han, C. D.; Park, J. C. Biomaterials 2001, 22, 219.
15. Cai, Q.; Wan, Y.; Bei, J. Z. Biomaterials 2003, 24, 3555.
16. Koji, N.; Yousuke, M.; Yuichi, O. Biomacromolecules 2007, 8, 2135.
17. Gao, Z.; Lukyanov, A. N.; Anurag Singhal, A.; Vladimir, P.; Torchilin, V. P. Nano Lett 2002, 2, 979.
18. Lukyanov, A. N.; Elbayoumi, T. A.; Chakilam, A. R.; Torchilin, V. P. J Controlled Release 2004, 100, 135.
19. Maedaa, N.; Takeuchia, Y.; Takada, M.; Sadzuka, Y.; Namba, Y.; Oku, N. J Controlled Release 2004, 100, 41.
20. Meijere, K.; Brezesinski, G.; Zschornig, O.; Arnold, K.; Mohwald, H. Phys Rev B: Condens Matter 1998, 248, 269.
21. Li, C. L.; Cui, J. X.; Wang, C. X.; Wang, J. X.; Li, Y. H.; Zhang, L.; Zhang, L.; Guo, W. M.; Wang, Y. L. Int J Pharm 2008, 362, 60.
22. Chen, H. L.; Yang, W. Z.; Chen, H.; Liu, L. R.; Gao, F. P.; Yang, X. D.; Jiang, Q.; Zhang, Q. Q.; Wang, Y. S. Colloids Surf B 2009, 73, 212.
23. Yu, H.; Guo, X. J.; Qi, X. L.; Liu, P. F.; Shen, X. Y.; Duan, Y. R. J Mater Sci Mater Med 2008, 19, 1275.
24. Wang, H.; Han, S. Y.; Sun, J. H.; Fan, T. F.; Tian, C. X.; Wu, Y. Carbohydr Polym 2011, 83, 1408.
25. Rodrigues, J. S.; Santos-Magalhaes, N. S.; Coelho, L. C. B. B.; Couvreur, P.; Ponchel, G.; Gref, R. J Controlled Release 2003, 92, 103.
26. Govender, T.; Stolnik, S.; Garnett, M. C.; Illum, L.; Davis, S. S. J Controlled Release 1999, 57, 171.
27. Sabesan, S.; Neria, S. Carbohydr Res 1992, 223, 169.
28. Lebouc, F.; Dez, I.; Madec, P. J. Polymer 2005, 46, 319.
29. Ubrich, N.; Bouillot, P. H.; Pellerin, C.; Hoffman, M.; Maincent, P. H. J. Controlled Release 2004, 97, 291.
30. Xu, J. X.; Tang, J. B.; Zhao, L. H. Acta Pharm Sinica 2009, 44, 1328.
31. Bae, Y.; Fukushima, S.; Harada, A.; Kataoka, K. Angew Chem Int Ed 2003, 42, 4640.